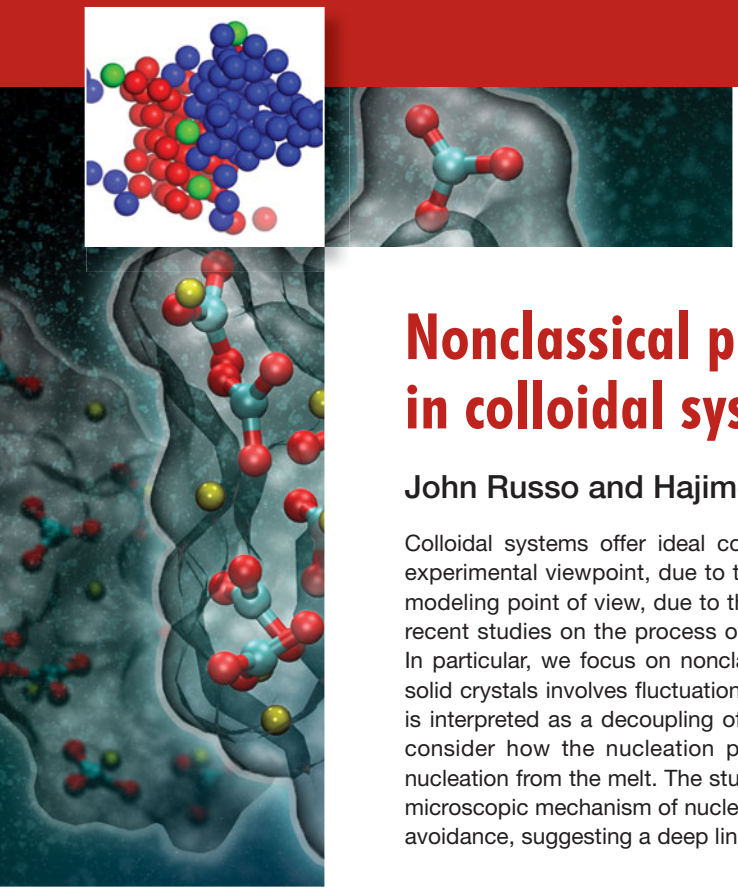


Nonclassical pathways of crystallization in colloidal systems

John Russo and Hajime Tanaka

Colloidal systems offer ideal conditions to study the nucleation process, both from an experimental viewpoint, due to their relatively large size and long time scales, and from a modeling point of view, due to the tunability of their interactions. In this article, we review recent studies on the process of colloidal crystallization from a microscopic perspective. In particular, we focus on nonclassical pathways to nucleation, where the appearance of solid crystals involves fluctuations of two or more order parameters. Nonclassical behavior is interpreted as a decoupling of positional and orientational symmetry breaking. We then consider how the nucleation pathway determines which polymorph is selected upon nucleation from the melt. The study of nucleation pathways not only sheds new light on the microscopic mechanism of nucleation, but also provides important information regarding its avoidance, suggesting a deep link between crystallization and vitrification.

Introduction

Nucleation is an important process, both for understanding the dynamics of first-order phase transitions and for practical applications, ranging from semiconductors, metals, chemicals, pharmaceutics, and the food industry, to studies of climate change. Despite a century of studies on nucleation (for a broad review, see Reference 1), the process is still not entirely understood, especially at a microscopic level. By far, the biggest problem with our classical understanding of nucleation is the small size of the crystalline nuclei involved in the transition (on the order of 10–1000 molecules in typical conditions). Such a small size casts doubt on the use of macroscopic thermodynamic properties in describing crystalline nuclei, for example, the use of surface tension in the presence of highly curved and rough interfaces of small nuclei. At the same time, it makes the observation of crystalline nuclei impractical for most atomic and molecular systems.

A notable class of systems in which the crystallization process is more easily accessible is colloidal suspensions. The size and the slow dynamics of typical colloidal suspensions allow for direct single-particle-level observations with confocal microscopy experiments.[2–6] Moreover, the tunability of their interactions makes them amenable to direct comparisons with simple soft matter models. For example, steric stabilization can be used to prevent colloidal particles from getting close to each other within the range of attractive forces, such that their phase behavior can be described by the ideal hard-sphere model. Colloidal systems can thus be considered as an ideal benchmark for testing our understanding of the nucleation theories. In this article, we review the recent progress in the field of colloidal crystallization, focusing on nonclassical pathways. These are identified as pathways in which different order parameters take distinct roles during the liquid-to-solid transition.

Beyond classical nucleation theory

The simplest and most general understanding of nucleation is embodied in classical nucleation theory (CNT), which provides a successful framework to understand and analyze data from nucleation for a large variety of processes.[1] However, its predictions are experimentally very difficult to test, especially given the exponential nature of the transition, which makes the results sensitive to small changes in experimental conditions. This difficulty is exemplified in nucleation studies of systems that, despite their simple interactions, have nucleation rates that are at odds with CNT.

An example is the condensation of argon,[7] where CNT predictions and experimentally measured rates differ by approximately 26 orders of magnitude. A second example involves the prototypical colloidal system, hard spheres (both poly(methyl methacrylate) and polystyrene microgel systems), where the discrepancy between predicted nucleation rates and

John Russo, Institute of Industrial Science, The University of Tokyo, Japan; and School of Mathematics, University of Bristol, UK; russoj@iis.u-tokyo.ac.jp
Hajime Tanaka, Institute of Industrial Science, The University of Tokyo, Japan; tanaka@iis.u-tokyo.ac.jp
doi:10.1557/mrs.2016.84

© 2016 Materials Research Society

https://doi.org/10.1557/mrs.2016.84 Published online by Cambridge University Press

experimental measurements is about 10 orders of magnitude. Numerical simulations found that the nucleation rate increases dramatically with the colloid volume fraction φ, growing by more than 15 orders of magnitude from φ = 0.52 to φ = 0.56, where it shows a maximum.[8–15]

On the other hand, experiments have found the nucleation rate to be much less sensitive to the volume fraction,[16,17] whose precise determination is also a challenging problem.[18] There have been several attempts at resolving this inconsistency, but a consensus has yet to be found. Two recent explanations have emerged. In the first,[19] the discrepancy is attributed to experiments, after noting that the gravitational lengths (i.e., the length scale over which the density profile changes due to gravity) of many of the colloidal samples are still very short compared to the size of the colloids. The basic idea is that the gravitational field coupled to long-range interactions (such as hydrodynamic interactions), can cause an increase in density fluctuations in the sample, triggering crystallization at a higher rate than that in the gravitation-free simulations. The second explanation attributed the discrepancy to the simulation conditions that neglect hydrodynamic interactions.[20] In the latter, hydrodynamic interactions have the effect of increasing the nucleation rate of colloids, thus potentially explaining the differences with experiments.

CNT rests on two main assumptions. The first is the so-called capillarity approximation, which assumes that small crystalline nuclei have the same thermodynamic properties as the bulk solid, such as specific volume or surface tension. However, many results contradict this assumption.[21,22] Several studies have attempted to go beyond the capillarity approximation. An account of these is beyond the scope of this article (see References 21–25).

The second assumption upon which CNT rests is that the process can be described by just one reaction coordinate—all order parameters involved in the transition proceed simultaneously. This assumption has also failed to capture the dynamics of the transition, especially in simulations where different reaction coordinates can be followed during nucleation.[26–31] Recent theoretical investigations are focusing on the extension of CNT to more than one dimension.[32,33]

Another assumption asserts that a supercooled liquid is homogeneous, and the nucleation happens randomly in space. Recent theoretical studies showed that this is not the case, even for quasi-single-component systems.[34] Effects of spatial heterogeneity also play an important role near a critical point, if it exists.[35] Thus, the effects of spatial heterogeneity of the melt should be taken into account.

Two-step nucleation and precursors

The inability of CNT to distinguish different pathways to crystallization, in which two or more order parameters evolve independently during the transition, has come to prominence with the discovery of two-step nucleation pathways.

Two-step crystallization refers to a nucleation pathway where, instead of direct nucleation from the gas phase (one-step crystallization), the system is found to crystallize inside disordered liquid droplets. These droplets usually form due to the presence of a metastable phase separation.[36–38] In colloidal systems, the process has been studied both experimentally[39,40] and theoretically.[35,41–44] The number and variety of solutions that have been found to crystallize from dense liquid precursors lead to the idea that two-step crystallization pathways are quite universal. For example, two-step crystallization processes have been suggested for systems outside the region of stability of the dense liquid phase, where a homogeneous fluid phase represents the stable thermodynamic state of the system.[38,41,45–48]

Perhaps the most surprising result is the suggestion that nucleation via dense amorphous regions can occur even in systems where a dense fluid phase does not exist. The best known example of such a system is given by colloidal models of hard spheres, whose crystallization behavior has been studied extensively.[2,8,10,13,30,49–51] For hard spheres, several observations have suggested that the presence of a metastable fluid–fluid demixing transition is not a necessary condition for a dense precursor-mediated crystallization process.[14,16,52–57] The role of density fluctuations and their priority over structural fluctuations are still subject to investigation, and for the moment, the importance of both contributions cannot be ruled out.[58] In the following, we focus on studies that, for colloidal systems with short-range interactions, point to an alternative nucleation pathway, where structural fluctuations, instead of density fluctuations, play a dominant role.

Two fundamental symmetries are broken at the liquid-to-solid transition: translational and orientational symmetry. Translational order is a measure of the positional order between a pair of particles in the system, while orientational order expresses the degree of angular order among three or more particles in the system. According to CNT, the crystallization process occurs in one step, with all the relevant order parameters changing at the same time across the transition. Two-step crystallization processes, instead, describe a scenario in which densification precedes structural ordering. The opposite scenario is also possible, with structural order fluctuations preceding the increase of density.

In order to study this process from a microscopic perspective, one should follow the nucleation process from the nucleation event to the growth of the crystalline nucleus over its critical nucleus size. By using local order parameters, describing the degree of translational[31,59] and orientational[8,31,60–62] order around individual particles, it is possible to construct a statistical map of the microscopic pathway to crystallization. While most of our knowledge comes from molecular simulations of model systems,[11,12,19,31,57,63] recent confocal microscope experiments using colloidal systems have also started to shed light on this process.[64,65]

Several investigations have suggested that the crystallization in hard sphere-like particles is first triggered by a structural (bond-orientational order) fluctuation, followed by densification of the ordered region. Evidence for this comes from the

https://doi.org/10.1557/mrs.2016.84 Published online by Cambridge University Press

study of the correlation length of fluctuations,[11,12,31,59,66,67] the lifetime of the fluctuations,[12,66–70] the radial profile of crystalline nuclei,[24,71] the Landau free energy profile,[31] and translational versus orientational curves.[31,59,64,65]

Evidence of bond-orientational foreshadowing of crystallization has been suggested for colloidal systems, both in simulations[11,12,31,59,63,72] and experiments.[64,65,73] Interestingly, the role of structural fluctuations has also been investigated in a variety of different systems, such as water,[74] metallic melts,[75,76] anisotropic particles,[77–79] and polymers.[80,81] The idea of studying crystallization under external fields (i.e., shear flow or external walls) by studying the effects of the field on the bond-orientational order is also a new direction for future research, whose power has been shown, for example, in Reference 82 for the case of crystallization in sheared suspensions. In this study, it was found that the crystallization rate has a nonlinear dependence on the shear intensity, which results from the suppression of bond-orientational ordered regions that are due to the shear flow.

Polymorph selection

Polymorph selection plays a fundamental role in many applications and has been the subject of many investigations.[30,31,63,83,84]

The observation that nucleation starts in regions of high bond-orientational order within the metastable fluid has important consequences in determining which polymorph is nucleating. We expect the structure of a particular crystal to reflect the symmetry of the precursor region from which it nucleated.

This idea was first tested in a colloidal hard-spheres fluid.[31] In hard spheres, the free-energy difference between the face-centered-cubic (fcc) and hexagonal close-packed (hcp) polymorphs is almost indistinguishable (approximately 0.1% of the thermal energy in favor of fcc).[85,86] This means that there is a comparable driving force for the nucleation of either the fcc or hcp crystal. Since fcc and hcp crystals are polytypes (meaning that they differ only in the stacking sequence along the direction perpendicular to the hexagonal planes), thermodynamics predicts random stacking between fcc and hcp planes (a crystal structure known as random close-packed structure). However, many studies, both experiments[2,6,49,87] and simulations,[10,31,88] have found that the fcc phase is much more abundant than the hcp phase. The preference for fcc nucleation can be understood by looking at the symmetry of the regions where nucleation occurs.

A study of the structural properties of supercooled hard spheres shows that the population of fcc-like precursor regions is bigger than the hcp-like precursor regions.[31] A convenient order parameter that distinguishes between fcc-like and hcp-like orientational symmetry is W_4: The fcc structure is characterized by negative values of W_4, while the hcp structure by positive values of W_4. **Figure 1** shows the probability distribution of the W_4 order parameter for precursor regions characterized by increasing values of bond-orientational order Q_6, which is a standard measure of bond-orientational order in spherically symmetric systems (see References 5 and 31 for a formal definition). While the supercooled melt has a symmetric distribution of W_4 (black curve), precursor regions progressively peak around negative values of W_4, indicating an fcc-like symmetry. The hcp-to-fcc transition would then occur at much longer time scales, due to the negligible free-energy difference between the two different polytypes.

Polymorph selection was also tested in the Gaussian core model (GCM), a model for the effective interaction between the centers of mass of polymers dispersed in a solvent.[89] The GCM has two different stable crystalline phases, a low-pressure fcc phase and a high-pressure bcc phase. The nucleation process in the GCM model was first considered, and it was shown that the description of the transition is enhanced by taking into account the prestructured particles surrounding the crystalline nucleus.[30] In a subsequent study, a clear link was established between the precursor regions and the crystal phase that nucleated from them, also noting a kinetic preference for the bcc phase, even in regions where the stable phase is fcc.[63] A later study found that the nuclei have a mixed nature, not consisting of just a single polymorph, and the kinetic pathway selected during nucleation persists even when the nucleus is many times above its critical size.[84] **Figure 2** shows an example of a mixed-phase nucleus. These results suggest that polymorph selection is already made in a supercooled state before nucleation starts, and it is connected to the symmetry of the precursor regions formed by structural fluctuations.

Slow dynamics and external fields

It is interesting to note that regions of high bond-orientational order have been linked not only to nucleation, but also to

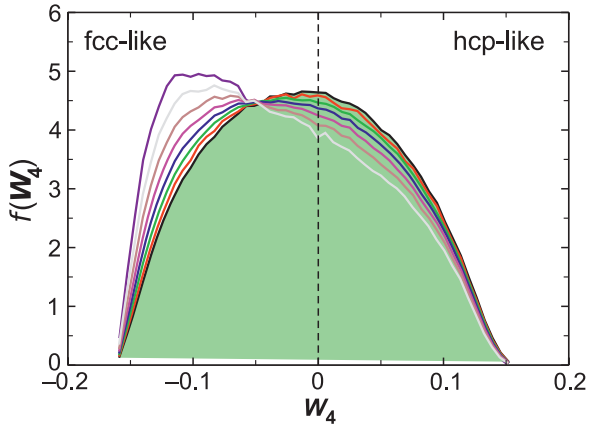


Figure 1. Origin of polymorph selection in a supercooled state. Hard spheres at reduced pressure $\beta P_s D^3 = 17$ ($\beta = 1/k_B T$, where k_B is the Boltzmann constant, T is the temperature, P_s is the pressure, and D is the diameter of the colloid): Probability distribution of the order parameter W_4 ($f(W_4)$) for sets of particles with increasing values of Q_6: 0.25, 0.26, 0.27, 0.28, 0.29, 0.30, 0.31, and 0.32. The full area (green shaded area) is the distribution for the melt, while increasing values of Q_6 skew the distribution toward the face-centered-cubic (fcc) symmetry. Note: hcp, hexagonal close-packed; Q_6, bond-orientational order parameter.

https://doi.org/10.1557/mrs.2016.84 Published online by Cambridge University Press

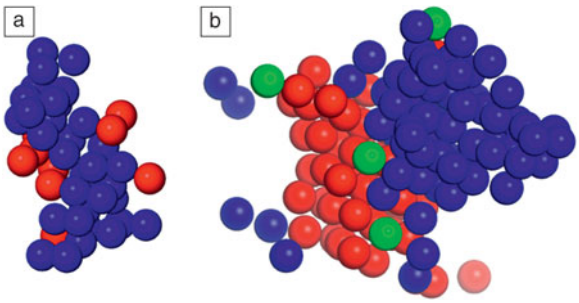


Figure 2. Gaussian core model at pressure P_s = 0.05 in units of k_BT/D^3. Two snapshots of the same nucleus as it grows. (a) Precritical nucleus and (b) post-critical nucleus. The blue particles are body-centered-cubic particles, green particles are hexagonal close-packed particles, and red particles are face-centered-cubic particles, showing a mixed-phase nucleus.

its absence (i.e., glass formation).[34] It was observed that over the time scale of heterogeneous dynamics (approximately comparable to the structural relaxation time), extended regions of high bond-orientational order displayed slower dynamics than disordered regions.[5,12,59,66,67,90,91] Apart from bond-orientational-ordered regions, highly packed regions are also characterized by slow dynamics.[5,59] The most notable of these structures is icosahedral packing, which since the pioneering work of Frank, is the archetypal model of amorphous structures. However, on approaching the glass transition, the icosahedral order does not grow in size, whereas bond-orientational order grows.[5,59] A link between slow dynamics and regions of extended bond-orientational order has been found in polydisperse hard spheres,[5,12,59,67] hard disks,[66,91,92] and colloidal ellipsoids.[93]

It has been shown that at high density, particles with icosahedral order outgrow the population of solid particles.[31] Even a small fraction of icosahedral particles strongly suppress the crystallization process.[94,95] The effect becomes more prominent with the introduction of polydispersity in particle size: It has been shown that the size asymmetry favors the formation of icosahedral environments, while suppressing the crystalline ones.[59]

Figure 3 shows the joint probability map of the order parameters q_4 and q_6. Different from Q_4 and Q_6, these order parameters have a spatial resolution that extends only to nearest neighbors and are thus suitable to detect icosahedral order, which cannot grow to form compact domains in space. This map is convenient because crystalline particles are located in the upper right corner of the map, while icosahedral-like environments are located in the upper left corner. We can see that, going from a system with 7% polydispersity (Figure 3a) to a system with 15% polydispersity (Figure 3b), the extent of crystalline regions is highly suppressed. It is interesting to note that disorder (in this case polydispersity) does not always destabilize the crystal. In the case of particles with angular (patchy) interactions, it was shown that angular disorder does not compromise the crystallizability of the system.[96]

Glasses are thermodynamically unstable, and, despite the slow dynamics, they can crystallize. The study of both the static[97] and dynamic[98] properties of the devitrification process holds great promise for the understanding of the glass transition.

Finally, we consider how an external field can couple with the orientational order in the fluid and affect its dynamics and crystallizability. This relationship was studied in a vertically vibrated quasi-two-dimensional granular liquid, and with polydisperse and bidisperse liquid Brownian simulations.[99] It was shown that the walls induce additional glassy order to the fluid, and this can be described by introducing a bond-orientational order correlation length that depends on the distance from the wall. With this simple modification, all scalings between static and dynamic length scales are the same as in the bulk. This also suggests a link between bond-orientational order and slow dynamics. Another study instead considered the effect of rough walls on colloidal suspensions under the effects of gravity,[19] and found that while rough walls do not perturb the density field, they strongly suppress bond-orientational order up to distances comparable to the

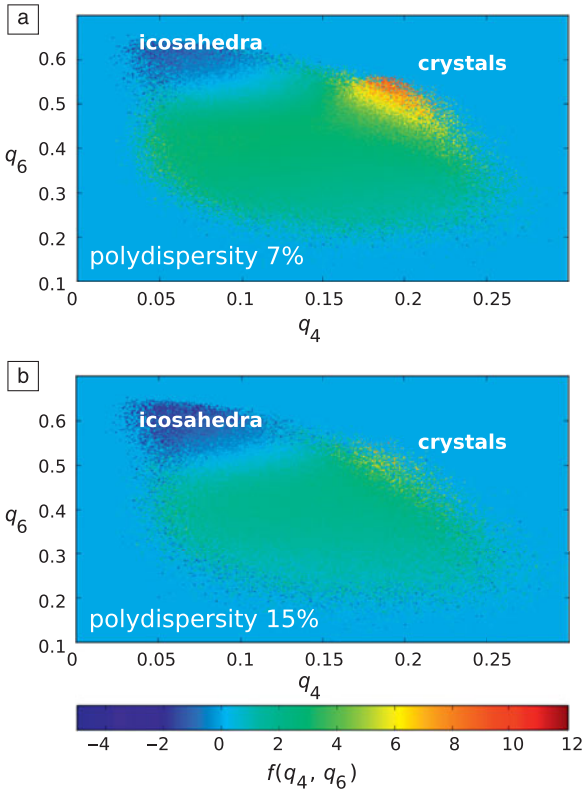


Figure 3. Effects of polydispersity on local structural ordering. (a) Polydisperse hard spheres at $\beta P_s D^3$ = 23: joint probability distribution $f(q_4, q_6)$ for 7% polydispersity. (b) Polydisperse hard spheres at $\beta P_s D^3$ = 23: joint probability distribution $f(q_4, q_6)$ for 15% polydispersity. The extent of crystalline regions is highly suppressed when polydispersity increases from 7% to 15%. Adapted from References 31, 59, and 63. Note: $\beta = 1/k_BT$, where k_B is the Boltzmann constant and T is the temperature; P_s, pressure; D, diameter of colloid.

https://doi.org/10.1557/mrs.2016.84 Published online by Cambridge University Press

bond-orientational correlation length. This suppression of bond-orientational order is then reflected in a strong suppression of nucleation close to the walls.

Another interesting external field is shear, which has been considered in detail in one study,[82] showing that shear suppresses the development of crystallization precursor regions, but favors the growth of crystal nuclei once they are formed. This offers a compelling explanation for the nonmonotonous dependence of the crystallization rate on the shear rate. The response of colloids to external fields makes them ideal candidates to uncover the effect of external fields on crystallization.[100]

Conclusion

We have reviewed recent progress on nonclassical pathways to crystallization in colloidal systems. Besides advancing our understanding of the nucleation process on a microscopic scale, these studies have shed light on interesting phenomena, such as polymorph selection, glassiness, and devitrification. For example, bond-orientational order plays a role also in glassy slow dynamics of a supercooled state of these systems, and colloidal systems are playing a fundamental role in linking structural information, accessible at single-particle resolution, with the microscopic dynamics. Especially interesting is the study of the effect of external fields on precursor regions and how this affects the nucleation process. Up to now, the case of external walls and uniform shear have been considered, but many other directions such as the effects on sedimentation are open to investigation.

References

1. K.F. Kelton, A.L. Greer, *Nucleation in Condensed Matter: Applications in Materials and Biology* (Elsevier, Amsterdam, 2010), vol. 15.
2. U. Gasser, E.R. Weeks, A. Schofield, P.N. Pusey, D.A. Weitz, *Science* **292**, 258 (2001).
3. H. Löwen, C.N. Likos, L. Assoud, R. Blaak, S. Van Teefelen, *Philos. Mag.* **87**, 847 (2007).
4. L. Assoud, F. Ebert, P. Keim, R. Messina, G. Maret, H. Löwen, *J. Phys. Condens. Matter* **21**, 464114 (2009).
5. M. Leocmach, H. Tanaka, *Nat. Commun.* **3**, 974 (2012).
6. J. Taffs, S.R. Williams, H. Tanaka, C.P. Royall, *Soft Matter* **9**, 297 (2013).
7. K. Iland, J. Wölk, R. Strey, D. Kashchiev, *J. Chem. Phys.* **127**, 154506 (2007).
8. S. Auer, D. Frenkel, *Nature* **409**, 1020 (2001).
9. E. Zaccarelli, C. Valeriani, E. Sanz, W.C.K. Poon, M.E. Cates, P.N. Pusey, *Phys. Rev. Lett.* **103**, 135704 (2009).
10. L. Filion, M. Hermes, R. Ni, M. Dijkstra, *J. Chem. Phys.* **133**, 244115 (2010).
11. T. Kawasaki, H. Tanaka, *Proc. Natl. Acad. Sci. U.S.A.* **107**, 14036 (2010).
12. T. Kawasaki, H. Tanaka, *J. Phys. Condens. Matter* **22**, 232102 (2010).
13. L. Filion, R. Ni, D. Frenkel, M. Dijkstra, *J. Chem. Phys.* **134**, 134901 (2011).
14. T. Schilling, S. Dorosz, H.J. Schöpe, G. Opletal, *J. Phys. Condens. Matter* **23**, 194120 (2011).
15. C. Valeriani, E. Sanz, P.N. Pusey, W.C.K. Poon, M.E. Cates, E. Zaccarelli, *Soft Matter* **8**, 4960 (2012).
16. S. Iacopini, T. Palberg, H.J. Schöpe, *J. Chem. Phys.* **130**, 084502 (2009).
17. M. Franke, A. Lederer, H.J. Schöpe, *Soft Matter* **7**, 11267 (2011).
18. C.P. Royall, W.C. Poon, E.R. Weeks, *Soft Matter* **9**, 17 (2013).
19. J. Russo, A.C. Maggs, D. Bonn, H. Tanaka, *Soft Matter* **9**, 7369 (2013).
20. M. Radu, T. Schilling, *Europhys. Lett.* **105**, 26001 (2014).
21. D.W. Oxtoby, *Acc. Chem. Res.* **31**, 91 (1998).
22. L. Gránásy, F. Iglói, *J. Chem. Phys.* **107**, 3634 (1997).
23. S. Prestipino, A. Laio, E. Tosatti, *Phys. Rev. Lett.* **108**, 225701 (2012).
24. F. Turci, T. Schilling, M.H. Yamani, M. Oettel, *Eur. Phys. J. Spec. Top.* **223**, 421 (2014).
25. J.F. Lutsko, *J. Chem. Phys.* **135**, 161101 (2011).
26. D. Moroni, P.R. ten Wolde, P.G. Bolhuis, *Phys. Rev. Lett.* **94**, 235703 (2005).
27. F. Trudu, D. Donadio, M. Parrinello, *Phys. Rev. Lett.* **97**, 105701 (2006).
28. B. Peters, B.L. Trout, *J. Chem. Phys.* **125**, 054108 (2006).
29. T. Zykova-Timan, C. Valeriani, E. Sanz, D. Frenkel, E. Tosatti, *Phys. Rev. Lett.* **100**, 036103 (2008).
30. W. Lechner, C. Dellago, P.G. Bolhuis, *Phys. Rev. Lett.* **106**, 085701 (2011).
31. J. Russo, H. Tanaka, *Sci. Rep.* **2**, 505 (2012).
32. S. Prestipino, A. Laio, E. Tosatti, *J. Chem. Phys.* **140**, 094501 (2014).
33. J.F. Lutsko, M.A. Durán-Olivencia, *J. Phys. Condens. Matter* **27**, 235101 (2015).
34. H. Tanaka, *Eur. Phys. J. E* **35**, 1 (2012).
35. P.R. ten Wolde, D. Frenkel, *Science* **277**, 1975 (1997).
36. D. Erdemir, A.Y. Lee, A.S. Myerson, *Acc. Chem. Res.* **42**, 621 (2009).
37. P.G. Vekilov, *Nanoscale* **2**, 2346 (2010).
38. D. Gebauer, M. Kellermeier, J.D. Gale, L. Bergström, H. Cölfen, *Chem. Soc. Rev.* **43**, 2348 (2014).
39. T.H. Zhang, X.Y. Liu, *J. Am. Chem. Soc.* **129**, 13520 (2007).
40. J. Savage, A.D. Dinsmore, *Phys. Rev. Lett.* **102**, 198302 (2009).
41. J.F. Lutsko, G. Nicolis, *Phys. Rev. Lett.* **96**, 46102 (2006).
42. K. Soga, J.R. Melrose, R.C. Ball, *J. Chem. Phys.* **110**, 2280 (1999).
43. J. Wedekind, L. Xu, S.V. Buldyrev, H.E. Stanley, D. Reguera, G. Franzese, *Sci. Rep.* **5**, 11260 (2015).
44. T. Haxton, L.O. Hedges, S. Whitelam, *Soft Matter* **11**, 9307 (2015).
45. O. Galkin, P.G. Vekilov, *Proc. Natl. Acad. Sci. U.S.A.* **97**, 6277 (2000).
46. P.G. Vekilov, *Cryst. Growth Des.* **4**, 671 (2004).
47. S. Chattopadhyay, D. Erdemir, J.M. Evans, J. Ilavsky, H. Amenitsch, C.U. Segre, A.S. Myerson, *Cryst. Growth Des.* **5**, 523 (2005).
48. R.P. Sear, *J. Chem. Phys.* **131**, 074702 (2009).
49. P.N. Pusey, W. van Megen, P. Bartlett, B.J. Ackerson, J.G. Rarity, S.M. Underwood, *Phys. Rev. Lett.* **63**, 2753 (1989).
50. J. Zhu, M. Li, R. Rogers, W. Meyer, R.H. Ottewill, STS-73 Space Shuttle Crew, W.B. Russel, P.M. Chaikin, *Nature* **387**, 883 (1997).
51. V.C. Martelozzo, A.B. Schofield, W.C.K. Poon, P.N. Pusey, *Phys. Rev. E* **66**, 021408 (2002).
52. H.J. Schöpe, G. Bryant, W. van Megen, *Phys. Rev. Lett.* **96**, 175701 (2006).
53. H.J. Schöpe, O. Marnette, W. van Megen, G. Bryant, *Langmuir* **23**, 11534 (2007).
54. H.J. Schöpe, G. Bryant, W. van Megen, *Phys. Rev. E* **74**, 060401 (2006).
55. H.J. Schöpe, G. Bryant, W. van Megen, *J. Chem. Phys.* **127**, 084505 (2007).
56. M. Franke, S. Golde, H.J. Schöpe, *Soft Matter* **10**, 5380 (2014).
57. T. Schilling, H.J. Schöpe, M. Oettel, G. Opletal, I. Snook, *Phys. Rev. Lett.* **105**, 25701 (2010).
58. J.T. Berryman, M. Anwar, S. Dorosz, T. Schilling, *Soft Condens. Matter* (2015), available at http://arxiv.org/abs/1503.07732.
59. M. Leocmach, J. Russo, H. Tanaka, *J. Chem. Phys.* **138**, 12A536 (2013).
60. P.J. Steinhardt, D.R. Nelson, M. Ronchetti, *Phys. Rev. B Condens. Matter* **28**, 784 (1983).
61. S. Auer, D. Frenkel, *Annu. Rev. Phys. Chem.* **55**, 333 (2004).
62. W. Lechner, C. Dellago, *J. Chem. Phys.* **129**, 114707 (2008).
63. J. Russo, H. Tanaka, *Soft Matter* **8**, 4206 (2012).
64. P. Tan, N. Xu, L. Xu, *Nat. Phys.* **10**, 73 (2014).
65. Y. Lu, X. Lu, Z. Qin, J. Shen, *Solid State Commun.* **217**, 13 (2015).
66. T. Kawasaki, T. Araki, H. Tanaka, *Phys. Rev. Lett.* **99**, 215701 (2007).
67. H. Tanaka, T. Kawasaki, H. Shintani, K. Watanabe, *Nat. Mater.* **9**, 324 (2010).
68. A. Malins, J. Eggers, C.P. Royall, S.R. Williams, H. Tanaka, *J. Chem. Phys.* **138**, 12A535 (2013).
69. A. Malins, J. Eggers, H. Tanaka, C.P. Royall, *Faraday Discuss.* **167**, 405 (2013).
70. C.P. Royall, S.R. Williams, *Phys. Rep.* **560**, 1 (2015).
71. M. Oettel, *J. Phys. Condens. Matter* **24**, 464124 (2012).
72. K. Kratzer, A. Arnold, *Soft Matter* **11**, 2174 (2015).
73. P.S. Mohanty, P. Bagheri, S. Nöjd, A. Yethiraj, P. Schurtenberger, *Phys. Rev. X* **5**, 011030 (2015).
74. J. Russo, F. Romano, H. Tanaka, *Nat. Mater.* **13**, 733 (2014).
75. R. Li, Y. Wu, J. Xiao, *J. Chem. Phys.* **140**, 034503 (2014).
76. T.T. Debela, X.D. Wang, Q.P. Cao, Y.H. Lu, D.X. Zhang, H.J. Fecht, H. Tanaka, J.Z. Jiang, *Phys. Rev. B Condens. Matter* **89**, 104205 (2014).
77. Y. Han, J. Lee, S.Q. Choi, M.C. Choi, M.W. Kim, *Phys. Rev. E* **88**, 042202 (2013).
78. N.A. Mahynski, A.Z. Panagiotopoulos, D. Meng, S.K. Kumar, *Nat. Commun.* **5**, 4472 (2014), doi:10.1038/ncomms5472.
79. C. Mondal, S. Karmakar, S. Sengupta, *J. Phys. Chem. B* **119**, 10902 (2015).
80. N.C. Karayiannis, K. Foteinopoulou, M. Laso, *Int. J. Mol. Sci.* **14**, 332 (2012).
81. R.S. Hoy, N.C. Karayiannis, *Phys. Rev. E* **88**, 012601 (2013).
82. B. Lander, U. Seifert, T. Speck, *J. Chem. Phys.* **138**, 224907 (2013).
83. C. Desgranges, J. Delhommelle, *J. Am. Chem. Soc.* **128**, 15104 (2006).
84. J.P. Mithen, A.J. Callison, R.P. Sear, *J. Chem. Phys.* **142**, 224505 (2015).

https://doi.org/10.1557/mrs.2016.84 Published online by Cambridge University Press

85. P.G. Bolhuis, D. Frenkel, S.C. Mau, D.A. Huse, *Nature* **388**, 235 (1997).
86. S. Pronk, D. Frenkel, *J. Chem. Phys.* **110**, 4589 (1999).
87. T. Palberg, *Curr. Opin. Colloid Interface Sci.* **2**, 607 (1997).
88. B. O'Malley, I. Snook, *Phys. Rev. Lett.* **90**, 85702 (2003).
89. C.N. Likos, *Soft Matter* **2**, 478 (2006).
90. H. Shintani, H. Tanaka, *Nat. Phys.* **2**, 200 (2006).
91. J. Russo, H. Tanaka, *Proc. Natl. Acad. Sci. U.S.A.* **112**, 6920 (2015).
92. T. Kawasaki, H. Tanaka, *J. Phys. Condens. Matter* **23**, 194121 (2011).
93. Z. Zheng, R. Ni, F. Wang, M. Dijkstra, Y. Wang, Y. Han, *Nat. Commun.* **5**, 3829 (2014).
94. H. Tanaka, *J. Phys. Condens. Matter* **15**, L491 (2003).
95. N.C. Karayiannis, R. Malshe, J.J. de Pablo, M. Laso, *Phys. Rev. E* **83**, 061505 (2011).
96. F. Romano, J. Russo, H. Tanaka, *Phys. Rev. Lett.* **113**, 138303 (2014).
97. T. Kawasaki, H. Tanaka, *Phys. Rev. E* **89**, 062315 (2014).
98. E. Sanz, C. Valeriani, E. Zaccarelli, W.C. Poon, M.E. Cates, P.N. Pusey, *Proc. Natl. Acad. Sci. U.S.A.* **111**, 75 (2014).
99. K. Watanabe, T. Kawasaki, H. Tanaka, *Nat. Mater.* **10**, 512 (2011).
100. K. Sandomirski, E. Allahyarov, H. Löwen, S.U. Egelhaaf, *Soft Matter* **7**, 8050 (2011). □

Two exciting conferences in one week!

Register by June 3 and SAVE!

DRC
74th Device Research Conference
June 19–22, 2016 // University of Delaware // Newark, DE
WWW.MRS.ORG/DRC-2016

EMC
58th Electronic Materials Conference
June 22–24, 2016 // University of Delaware // Newark, DE
WWW.MRS.ORG/58TH-EMC

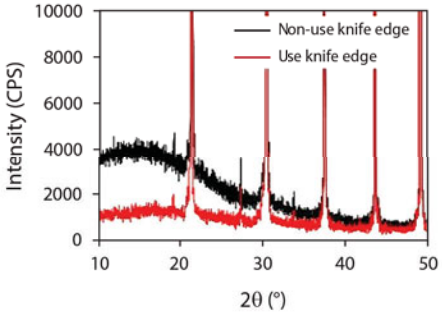
Rigaku
Leading With Innovation

XRD WITH VARIABLE KNIFE EDGE FEATURE

Rigaku MiniFlex300/600 can be equipped with the D/teX Ultra high-speed 1-dimensional detector to obtain greater intensity. This detector has a broad detection surface and can efficiently count diffraction X-rays from a sample. As a result, it is possible to obtain intensities from a few tens to roughly 100 times greater than a scintillation counter. Background can also be reduced using the fluorescent X-ray reduction mode or the knife edge feature. The figure shows the X-ray diffraction patterns obtained when a knife edge is installed versus no knife edge. By using a knife edge, it is possible to achieve an extreme reduction in scattering on the low-angle side. Also, the knife edge moves in a way which is dependent on the diffraction angle 2θ, and thus there is no blind spot (intensity attenuation) on the high-angle side, and measurement can be done from the low-angle side to the high-angle side.

MiniFlex

X-ray diffraction patterns (enlarged) of zeolite, measured when a knife edge is installed versus no knife edge.





APPBYTE

Rigaku Corporation and its Global Subsidiaries
www.Rigaku.com | info@Rigaku.com

https://doi.org/10.1557/mrs.2016.84 Published online by Cambridge University Press